Med Chem Res
DOI 10.1007/s00044-017-2098-0

MEDICINAL CHEMISTRY RESEARCH

ORIGINAL RESEARCH

Synthesis and pharmacological evaluation of pyridinyl-1,3,4-oxadiazolyl-ethanone derivatives as antimicrobial, antifungal and antitubercular agents

Mohammad Hashim Mansoori[1] · Gopal L. Khatik[2] · Vijay Mishra[3]

Received: 12 June 2017 / Accepted: 12 October 2017

Abstract Nicotinic acid was converted into different substituted acetylated nicotinic acid derivatives by sequential transformation involving formation of hydrazide, Schiff's base and finally acylated oxadiazole derivatives. The synthesized compounds were characterized by spectroscopic techniques and evaluated in vitro for the antimicrobial, antifungal, as well as antitubercular activity. Among all the synthesized derivatives, compounds **6b**, **6d**, **6e**, **6g**, and **6j** demonstrated excellent antimicrobial activity on *Bacillus subtilis*. The compounds **6d**, **6j** and compounds **6b**, **6f**, **6h**, and **6i** exhibited maximum zone of inhibition against fungi *Candida albicans* as well as *Aspergillus niger*, respectively at the concentration of 500 µg/mL. The antitubercular activity exhibited by **6f**, **6g**, and **6d** with minimum inhibitory concentration (MIC) values of 1.2, 3.1, and 7.8 µg/mL, respectively. The synthesized compounds were studied by molecular docking through Autodock Vina to evaluate their interaction at respective proteins. Further the effect of synthesized derivatives on surface morphology of human erythrocytes as well as hemolysis was also evaluated. The results demonstrated lesser extent of hemolytic toxicity.

Graphical abstract

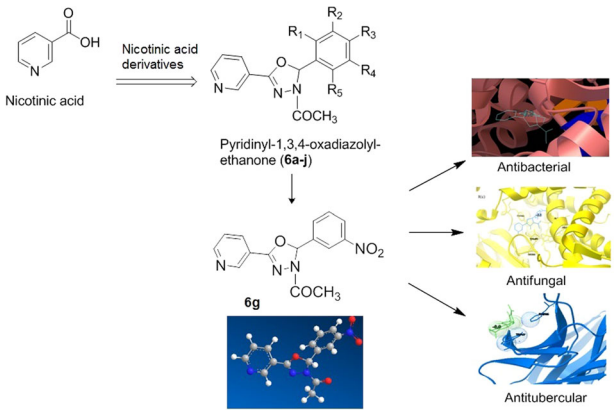

Keywords Tuberculosis · Nicotinic acid · Schiff base · Antibacterial activity · Antifungal activity · Hemolytic toxicity

Introduction

Currently microbial diseases are major concern due to developing resistance against the existing antimicrobial agents. Among the microbial diseases bacterial and fungal infections are more likely to cause the high rate of morbidity and mortality worldwide. Tuberculosis (TB), a respiratory transmitted disease representing a formidable challenge to global public health, is caused by the infection with various strains of the air-born pathogen of genus *Mycobacterium*

Electronic supplementary material The online version of this article (https://doi.org/10.1007/s00044-017-2098-0) contains supplementary material, which is available to authorized users.

✉ Vijay Mishra
vijaymishra2@gmail.com
vijay.20352@lpu.co.in

[1] Department of Medicinal Chemistry, Adina Institute of Pharmaceutical Sciences, Sagar, MP 470002, India

[2] Department of Pharmaceutical Chemistry, Lovely Institute of Technology (Pharmacy), Lovely Professional University, Phagwara, Punjab 144411, India

[3] Department of Pharmaceutics, Lovely Institute of Technology (Pharmacy), Lovely Professional University, Phagwara, Punjab 144411, India

Published online: 20 October 2017

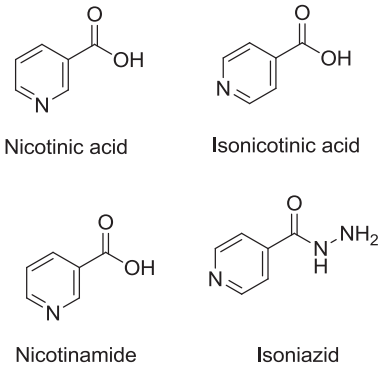

Fig. 1 Nicotinic acid, isonicotinic acid and its antimicrobial derivative (isoniazid)

mainly *Mycobacterium tuberculosis* (*M. tbc*) (Nookala and Subash 2013). In 2015, as per World Health Organization (WHO) statistics, an estimated 10.4 million new TB cases and 1.4 million TB deaths were reported worldwide. During the period of year 2000 and 2015, the deaths due to TB cut down by 22%, however TB stayed as one of the top 10 causes of death worldwide in 2015 (WHO 2015).

Although a number of drugs are available for the treatment of TB but most of them fail to treat TB completely, because the interruption of antibiotics course and insufficient level of drug in the body are unable to kill 100% of mycobacteria. Among all the drugs, high-dose of isoniazid, pyrazinamide, and ethambutol (the first-line drugs) are the first choice for the treatment of TB, while fluoroquinolones (levofloxacin, ciprofloxacin, ofloxacin) are the second choice (Slayden et al. 2000; Caminero et al. 2010), but isoniazid and floroquinolones have limited use due to its hepatotoxicity and nephrotoxicity. These drawbacks suggest that the design of newer and more potent antitubercular (anti-TB) drugs with minimal toxic effects for improved treatment of drug-resistant and drug-sensitive TB is imperative (Punkvang et al. 2010).

From the past few decades the chemical research revealed that the nicotinic acid (pyridine-3-carboxylic acid) and isonicotinic acid (pyridine-4-carboxylic acid) derivatives like isoniazid (Fig. 1), a well known anti-TB drug showed potent antimicrobial activity (Jo et al. 2004; Lourenço et al. 2007; Navarrete-Vázquez et al. 2007; Desai et al. 2008).

The present investigation was aimed to find out newer acetylated derivatives of nicotinic acid with potent antibacterial, antifungal, and antitubercular activities.

Materials and methods

Chemistry

The synthesized compounds were purified by thin layer chromatography technique using a solvent system consisting chloroform and methanol in 1:1 ratio. All chemicals used were of analytical grade purchased from respective manufacturers. Open capillary method was employed for the determination of melting points and were uncorrected.

Fourier transformed infrared spectroscopic data was recorded on spectrophotometer (Perkin Elmer 783, Pyrogen 1000 Spectrophotometer, USA) employing KBr disc method. Mass spectra of all the synthesized compounds were recorded on a JEOL GC Mass spectrometer (Japan). The ^{1}H nuclear magnetic resonance (NMR) spectra of the synthesized acetylated schiffs base of nicotinic acid were recorded in terms of chemical shifts (δ, ppm) on JEOL GSX 400 spectrometer (Japan) using trimethyl silaxane as internal standard and dimethyl sulphoxide (DMSO) as solvent (Supplementary data).

General procedure of Schiff's base

Mixture of nicotinic acid (0.03 mol, 1.0 equiv) and PCl_5, (0.05 mL, 1.5 equiv) in 20 mL anhydrous CCl_4 was refluxed for 2 h. Solvent was distilled off and nicotinoyl chloride was obtained (Navarrete-Vázquez et al. 2007). Further the hydrazine hydrate (0.1 mol, 3.3 equiv) was added in nicotinoyl chloride (0.03 mol, 1.0 equiv) drop wise at 0 °C, the resultant mixture was separated out and washed with aqueous sodium carbonate (10% w/v) and dried under vacuum. The crystalline nicotinoyl hydrazide was obtained by recrystallization with methanol (Kalia et al. 2007). Further nicotinoyl hydrazide (0.01 mol, 1.0 equiv) and aromatic aldehyde (0.01 mol, 1.0 equiv) were mixed in tetrahydrofuran (25 mL) and heated gently for 2 h at 60 °C. The reaction mixture was then poured into ice cold water and filtered. The pure compound, Schiff base was obtained by recrystallization with methanol (Boovanahalli et al. 2007).

Synthesis of acetylated nicotinic acid derivatives (6a–j)

Acetic anhydride (10 mL) and Schiff base (0.01 mol) were dissolved in 25 mL of ethanol and refluxed for 2 h. Then reaction mixture was concentrated and allowed to cool resulting in acetylated product, which was filtered, washed with water and recrystallized using methanol (Pandey et al. 2005). This final step resulted in the synthesis of different acetylated nicotinic acid derivatives (compounds **6a–j**) (Table 1), which were characterized using various spectroscopic techniques.

*1-(2-Phenyl-5-(Pyridin-3-yl)-1,3,4-oxadiazole-3 (2H)-yl) ethanone (**6a**)*

Yield: 62%; mp 145–147 °C; IR (KBr) ν_{max} 3009, 2901, 1686, 1602, 1584, 1329, 1323 cm^{-1}: ^{1}H NMR (DMSO-d$_6$,

Table 1 Synthesis of nicotinic acid derivatives (**6a–j**)

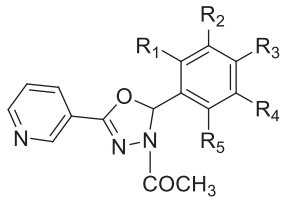

6a-j

Synthesized compounds	R_1	R_2	R_3	R_4	R_5	Yield (%)
6a	H	H	H	H	H	62
6b	H	H	$N(CH_3)_2$	H	H	65
6c	H	H	H	H	Cl	63
6d	H	H	H	H	NO_2	67
6e	H	H	OCH_3	H	H	61
6f	H	Cl	NO_2	H	H	68
6g	H	H	H	NO_2	H	66
6h	H	H	OH	OCH_3	H	64
6i	H	H	CH_3	H	H	65
6j	H	OCH_3	OCH_3	H	H	63

400 MHz): 7.3–9.2 (m, 9H), 8.1 (s, 1H), 2.4 (s, 3H); ^{13}C NMR (DMSO-d_6, 100 MHz) δ: 23.4 (CH_3), 74.5 (CH), 123.9 (CH), 126.3 (C), 126.8 (CH), 127.0 (CH), 128.6 (CH), 137.2 (CH), 140.4 (C), 151.5 (CH), 152.0 (CH), 155.0 (C), 168.6 (C); EIMS *m/z* 267.17 (M^+); Anal $C_{15}H_{13}N_3O_2$ calcd. C, 67.4, H, 4.9, N, 15.72. Found C, 67.1, H, 4.6, N, 15.64.

*1-(2-(4-dimethylamino)phenyl)-5-(pyridine-3-yl)-1,3,4-oxadiazole-3(2H)-yl) ethanone (**6b**)*

Yield: 65%; mp 170–172 °C; IR (KBr) ν_{max}: 3080, 2924, 1701, 1632, 1597, 1421, 1361 cm^{-1}; ^{1}H NMR (DMSO-d_6, 400 MHz): 6.6–9.2 (m, 8H), 8.1 (s, 1H), 2.4 (s, 3H), 2.9 (s, 6H); ^{13}C NMR (DMSO-d_6, 100 MHz) δ: 23.4 (CH_3), 40.3 (CH_3), 74.5 (CH), 114.1 (CH), 123.9 (CH), 126.3 (C), 127.9 (CH), 129.9 (CH), 137.2 (CH), 147.6 (C), 151.5 (CH), 152.0 (CH), 155.0 (C), 168.6 (C); EIMS *m/z* 310.25 (M^+); Anal $C_{17}H_{18}N4O_2$ calcd. C, 65.79, H, 5.85, N, 18.05. Found C, 65.68, H, 5.76, N, 18.02.

*1-(2-(2-chlorophenyl)-5-(pyridine-3-yl)-1,3,4-oxadiazole-3(2H)-yl) ethanone (**6c**)*

Yield: 63%; mp 180–182 °C; IR (KBr) ν_{max}:: 3058, 2885, 1673, 1638, 1594, 1419, 1360, 762 cm^{-1}; ^{1}H NMR (DMSO-d_6, 400 MHz): 7.2–9.2 (m, 8H), 8.1 (s, 1H), 2.4 (s, 3H); ^{13}C NMR (DMSO-d_6, 100 MHz): δ: 23.4 (CH_3), 65.4 (CH), 123.9 (CH), 126.3 (C), 126.7 (CH), 128.2 (CH), 128.4 (CH), 128.7 (CH), 132.3 (C), 137.2 (CH), 142.8 (C), 151.5 (CH), 152.0 (CH), 155.0 (C), 168.6 (C); EIMS *m/z* 301.51 (M^+); Anal $C_{15}H_{12}ClN_3O_2$ calcd. C, 59.71, H, 4.01, N, 13.93. Found C, 59.68, H, 4.0, N, 35.84.

*1-(2-(2-Nitrophenyl)-5-(pyridine-3-yl)-1,3,4-oxadiazole-3(2H)-yl) ethanone (**6d**)*

Yield: 67%; mp 189–191 °C; IR (KBr) ν_{max}:: 3029, 2849, 1669, 1651, 1593, 1420, 1343 cm^{-1}; 1H NMR (DMSO-d_6, 400 MHz): 7.6–9.2 (m, 8H), 8.1 (s, 1H), 2.4 (s, 3H); 13C NMR (DMSO-d_6, 100 MHz) δ: 23.4 (CH_3), 65.9 (CH), 120.9 (CH), 123.9 (CH), 126.3 (C), 127.7 (CH), 127.9 (CH), 134.7 (CH), 137.2 (CH), 137.5 (C), 147.0 (C), 151.5 (CH), 152.0 (CH), 155.0 (C), 168.6 (C); EIMS *m/z* 312.71 (M+); anal $C_{15}H_{12}N_4O_4$ calcd. C, 57.69, H, 3.87, N, 17.94. Found C, 57.61, H, 3.82, N, 17.83.

*1-(2-(4-Methoxyphenyl)-5-(pyridine-3-yl)-1,3,4-oxadiazole-3(2H)-yl) ethanone (**6e**)*

Yield: 61%; mp 173–175 °C; IR (KBr) ν_{max} cm^{-1}: 3072, 2924, 1701, 1632, 1597, 1421, 1361, 1293 cm^{-1}; ^{1}HNMR (DMSO-d_6, 400 MHz): 6.8–9.2 (m, 8H), 8.1 (s, 1H), 2.4 (s, 3H), 3.7 (s, 3H); ^{13}C NMR ((DMSO-d_6, 100 MHz) δ: 23.4 (CH_3), 55.9 (CH_3), 74.5 (CH), 114.1 (CH), 123.9 (CH), 126.3 (C), 132.7 (C), 137.2 (CH), 151.5 (CH), 152.0 (CH), 155.0 (C), 158.7 (C), 168.6 (C); EIMS *m/z* 297.33 (M^+);

anal $C_{16}H_{15}N_3O_3$ calcd. C, 64.64, H, 5.09, N, 14.13. Found C, 64.56, H, 5.06, N, 14.08.

*1-(2-(3-Chloro-4-nitrophenyl)-5-(pyridine-3-yl)-1,3,4-oxadiazole-3(2H)-yl) ethanone (**6f**)*

Yield: 68%; mp 182–184 °C; IR (KBr) ν_{max}: 3000, 2900, 1700, 1640, 1596, 1468, 1423, 1375, 738 cm^{-1}; ^1H NMR (DMSO-d_6, 400 MHz): 7.6–9.2 (m, 7H), 8.1 (s, 1H), 2.4 (s, 3H); ^{13}C NMR (DMSO-d_6, 100 MHz) δ: 23.4 (CH_3), 74.0 (CH), 122.3 (CH), 123.9 (CH), 126.0 (CH), 126.3 (C), 127.7 (CH), 128.7 (C), 137.2 (CH), 151.5 (CH), 152.0 (CH), 155.0 (C), 146.8 (C), 147.9 (C), 168.6 (C); EIMS *m/z* 346.22 (M^+); anal $C_{15}H_{11}ClN_4O_4$ calcd. C, 51.96, H, 3.2, N, 16.16. Found C, 51.85, H, 3.1, N, 16.04.

*1-(2-(3-Nitro-phenyl)-5-pyridine-3-yl-(1,3,4) oxadiazol-3-yl) ethanone (**6g**)*

Yield: 66%; mp 191–193 °C; IR (KBr) ν_{max}: 3195, 2923, 1682, 1651, 1596, 1475, 1387 cm^{-1}; 1H NMR (DMSO-d_6, 400 MHz): 7.2–9.2 (m, 8H), 8.1 (s, 1H), 2.4 (s, 3H); 13C NMR (DMSO-d_6, 100 MHz) δ: 23.4 (CH_3), 73.5 (CH), 119.1 (CH), 122.2 (CH), 123.9 (CH), 126.3 (C), 129.5 (CH), 133.1 (CH), 137.2 (CH), 141.3 (C), 148.2 (C), 151.5 (CH), 152.0 (CH), 155.0 (C), 168.6 (C); EIMS *m/z* 312.88 (M+); anal $C_{15}H_{12}N_4O_4$ calcd. C, 57.69, H, 3.87, N, 17.94. Found C, 57.61, H, 3.79, N, 17.85.

*1-(2-(4-Hydroxy-3-methoxyphenyl)-5-(pyridine-3-yl)-1,3,4-oxadiazole-3(2H)-yl)ethanone (**6h**)*

Yield: 64%; mp 150–152 °C; IR (KBr) ν_{max}: 3383, 3063, 2957, 1698, 1651, 1596, 1475, 1374, 1304, 1202 cm^{-1}; ^1H NMR (DMSO-d_6, 400 MHz): 7.6–9.2 (m, 7H), 8.1 (s, 1H), 2.4 (s, 3H), 2.1 (s, 1H), 3.8 (s, 3H);^{13}C NMR (DMSO-d_6, 100 MHz) δ: 23.4 (CH_3), 56.2 (CH_3), 74.8 (CH), 112.4 (CH), 116.7 (CH), 120.7 (CH), 123.9 (CH), 126.3 (C), 134.0 (C), 137.2 (CH), 143.7 (C), 151.2 (C), 151.5 (CH), 152.0 (CH), 155.0 (C), 168.6 (C); EIMS *m/z* 313.09 (M^+); anal $C_{16}H_{15}N_3O_4$ calcd. C, 61.34, H, 4.83, N, 13.41. Found C, 61.24, H, 4.76, N, 13.34.

*1-(5-Pyridine-3-yl)-2-p-tolyl-1,3,4-oxadiazole-3(2H)-yl) ethanone (**6i**)*

Yield: 65%; mp 157–159 °C; IR (KBr) ν_{max}: 3212, 3010, 1699, 1636, 1574, 1418, 1361, 1293 cm^{-1}; ^1H NMR (DMSO-d_6, 400 MHz): 7.3–9.2 (m, 8H), 8.1 (s, 1H), 2.3 (s, 3H), 2.4 (s, 3H); ^{13}C NMR (DMSO-d_6, 100 MHz) δ: 23.4 (CH_3), 24.3 (CH_3), 74.5 (CH), 123.9 (CH), 126.9 (CH), 126.3 (C), 128.9 (CH), 136.4 (C), 137.2 (CH), 151.5 (CH), 152.0 (CH), 155.0 (C), 168.6 (C); EIMS *m/z* 281.42 (M^+); anal $C_{16}H_{15}N_3O_2$ calcd. C, 68.31, H, 5.37, N, 14.94. Found C, 68.26, H, 5.15, N, 14.67.

*1-(2-(3,4-Dimethoxyphenyl)-5-(pyridine-3-yl)-1,3,4-oxadiazole-3(2H)-yl) ethanone (**6j**)*

Yield: 63%; mp 140–142 °C; IR (KBr) ν_{max}:: 3210, 2915, 1698, 1652, 1596, 1417, 1373, 1301 cm^{-1}; ^1H NMR (DMSO-d_6, 400 MHz): 7.5–9.2 (m, 7H), 8.1 (s, 1H), 2.4 (s, 3H), 3.6 (s, 6H); ^{13}C NMR (DMSO-d_6, 100 MHz) δ: 23.4 (CH_3), 56.2 (CH_3), 74.8 (CH), 112.2 (CH), 115.1 (CH), 120.3 (CH), 123.9 (CH), 126.3 (C), 133.7 (C), 137.2 (CH), 147.8 (C), 149.6 (C), 151.5 (CH), 152.0 (CH), 155.0 (C), 168.6 (C); EIMS *m/z* 327.92 (M^+); Anal $C_{17}H_{17}N_3O_4$ calcd. C, 62.38, H, 5.23, N, 12.84. Found C, 62.29, H, 5.11, N, 12.74.

Antimicrobial activity

The cup-plate method was adopted in the present investigation. Briefly, the nutrient agar medium, containing standard bacterial inoculums was filled in cups or disks of standard diameter. After introducing the test compounds into the disks, the diameter of zone of inhibition was measured. All synthesized compound were dissolved in dimethyl formamide (DMF) to form the concentration of 125, 250, and 500 µg/mL. Ciprofloxacin and ketoconazole were used as the standard for antibacterial and antifungal studies, respectively.

Antibacterial activity

Different microorganisms like *S. aureus*, *B. aureus*, *E. coli*, and *P. aeruginosa* used for determining the anti-bacterial activity of synthesized compounds were confirmed by biochemical test and maintained on nutrient agar (Muller Hinton Agar, HiMedia, Mumbai) slopes at pH 7.4. Briefly the required amount of test solution (40 µL of each tested concentration of synthesized compounds) and standard solution (40 µL) were added into each cup and kept undisturbed for at least 2 h at room temperature to allow proper diffusion of the test and standard solution into the nutrient agar medium. The petri plates were incubated at 37 ± 1 °C for 24 h and the diameter of zone of inhibition was measured. Simultaneously controls were maintained using DMF for the observation of solvent effects.

Antifungal activity

Fungi *C. albicans* and *A. niger* were employed for the estimation of antifungal activity of synthesized compounds. Sabouraud dextrose agar (SDA; HiMedia, Mumbai) was used for the cultivation of fungi, particularly pathogenic

fungi associated with skin infections. The 40 µL of solution of each test compounds at the concentration of 125, 250, and 500 µg/mL prepared in DMF was placed in the cups under laminar air flow. The DMF and Ketoconazole were used as control and standard, respectively. Zones of inhibition (mm) were measured after 24 h of incubation.

In vitro antitubercular activity

Microplate Alamar Blue Assay (MABA) was used to determine the antimycobacterial activity of the synthesized compounds. Briefly, 100 mL of Middle brook 7H9 broth (Difco, Detroit, USA) supplemented with 0.2% glycerol, OADC (oleic acid, albumin, dextrose, catalase), and 0.05% Tween 80 (Complete medium was referred as 7H9GC-T80) was used to inoculate bacterial strains *M. tuberculosis* H37Rv (ATCC 27294). Rifampicin was used as positive control. Minimum inhibitory concentration (MIC) was determined post 7 days incubation at 37 ± 1 °C. For minimizing the background fluorescence Anti-TB susceptibility testing was executed in black, clear-bottomed 96-well microplates. Initial dilutions of synthesized compound were prepared in DMSO and 0.1 mL of H12 media in microplates was used for subsequent two fold dilutions. The H37 Rv was diluted in 7H9 media to reach approximately 2×10^5 cfu/mL and 0.1 mL was added to wells. At 7th day of incubation, 20 µL of Alamar Blue solution and 12.5 mL of 20% Tween 80 were added to all the wells and plates were re-incubated for 24 h. For measuring fluorescence Victor II multilabel fluorometer (Perkin Elmer Life Sciences Inc., Boston, MA) was operated at 530 and 590 nm. The MIC was taken as the lowest drug concentration affecting an inhibition of ≥ 90% and percent inhibition was determined by following equation (Table 2) (Lourenço et al. 2007; Kamanna and Kashyap 2007)-

$$\text{Percent inhibition} = 1 - (\text{test well FU}/\text{mean FU of triplicate B wells}) \times 100 \quad (1)$$

Table 2 In vitro antitubercular activity of synthesized compounds (**6a–j**)

Entry	Compounds	% Inhibition (100 µg/mL)	MIC (µg/mL)
1	**6a**	101	10.4
2	**6b**	101	8.6
3	**6c**	100	11.7
4	**6d**	101	7.8
5	**6e**	48	>100
6	**6f**	101	1.2
7	**6g**	100	3.1
8	**6h**	98	53.9
9	**6i**	78	>100
10	**6j**	101	46.3
11	Rifampicin	100	0.0047

Test concentration: 100 µg/mL; strain: *M. tuberculosis* H37Rv; method: MABA; stock concentration: 10 mg/mL

Evaluation of effect on surface morphology of human erythrocytes

This study was performed to evaluate whether the synthesized compounds exhibited any detrimental effect on the surface morphology of human erythrocytes. This study was performed according to the previously reported method, with slight modification (Mishra et al. 2010). Briefly, blood of a healthy donor obtained from a local blood bank was kept in a blood collection tube (Piove Di Sacco, Italy) containing K_3 EDTA anticoagulant. Erythrocytes separated by centrifugation were washed with phosphate buffer saline (PBS) pH 7.4 and resuspended in PBS pH 7.4. Erythrocytes were used immediately after isolation. Suspension of erythrocytes in PBS was treated with different synthesized compounds at a fixed concentration (1 mg/mL). Then cell samples were viewed under a Leica optical microscope (Leica, DMLB, Switzerland) using a magnification of 400× for the morphological condition of erythrocytes (Mishra and Jain 2014).

In vitro hemolytic toxicity

For studying the effects of synthesized compounds on the lysis of erythrocytes, the suspension of erythrocytes (0.1 mL; 10% hematocrit value) and synthesized compounds (0.9 mL; 1 mg/mL in PBS, pH 7.4) were incubated for 30 min at 37 ± 1 °C and then the mixtures were centrifuged at 3000 rpm for 10 min to remove nonlysed erythrocytes. The supernatant was analyzed spectrophotometrically (1601 UV–Vis spectrophotometer, Shimadzu, Japan) at 540 nm ($n = 6$). To obtain 0 and 100% hemolysis, erythrocytes suspension (0.1 mL) was mixed with NaCl solution (0.9 mL; 0.9% *w/v*) and distilled water (0.9 mL), respectively (Mishra et al. 2010; Mishra and Jain 2014). The degree of hemolysis was determined by using the following equation:

$$\text{Hemolysis}(\%) = (\text{AbsS} - \text{Abs0})/(\text{Abs100} - \text{Abs0}) \times 100 \quad (2)$$

where AbsS, Abs0, and Abs100 are the absorbance of sample, a solution showing 0% hemolysis and a solution showing 100% hemolysis, respectively.

Molecular modeling

For the identification of potentially active ligands, the designed molecules were analyzed by molecular docking

using Autodock Vina 1.5.6 software, a molecular docking software (Trott and Olson 2010; Chaurasiya et al. 2016; Kaur and Khatik 2016; Khatik et al. 2011, 2012). For the extraction and preparation of ligands, the desired proteins were downloaded from protein data bank (www.rcsb.org/pdb/home/home.do). The selected protein was validated by the extraction of ligand and docking it in a same manner as actual ligand. For preparation of protein it was reloaded and various problems were fixed such as missing bonds or atoms, and removed extraneous structures like water molecules. Polar hydrogens were added along with the Kollaman charges. After saving the macromolecule (as pdbqt file) the ligand.pdbqt was loaded and set it as map type by choosing ligand and grid box was generated. The compounds were drawn by ChemDraw Ultra and converted to 3D structures. Geometry of all compounds was optimized by semiemperical MM2 method. Molecular docking was performed on optimized structure of protein.

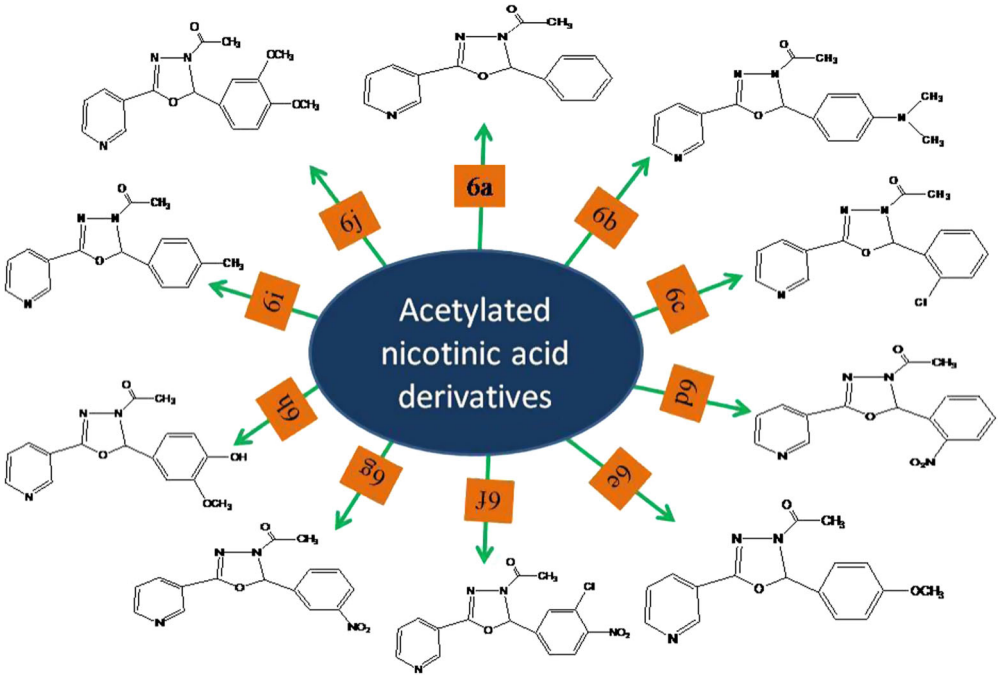

Fig. 2 Pictorial representation of synthesized nicotinic acid derivatives (**6a–j**)

Scheme 1 Synthesis of acetylated nicotinic acid derivatives

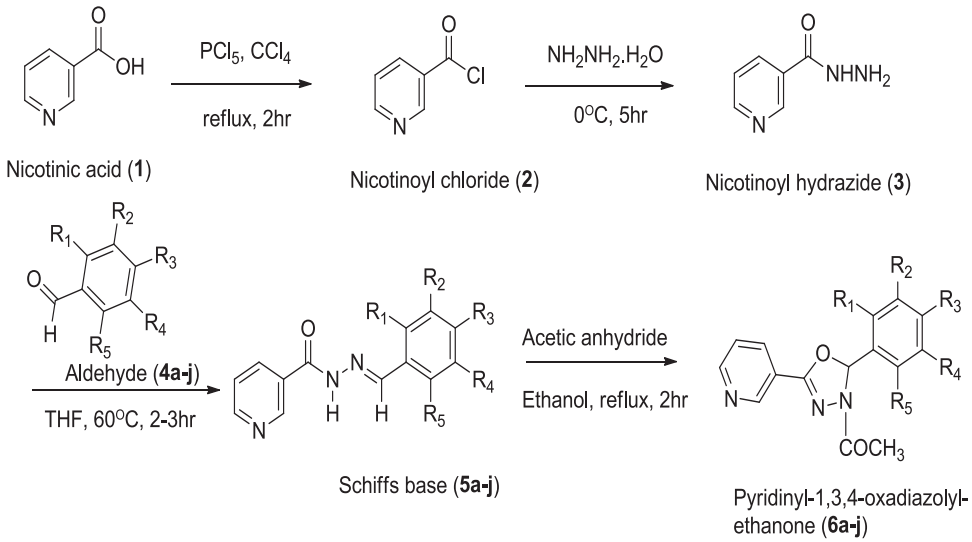

Results and discussion

Chemistry

Different acetylated nicotinic acid derivatives (**6a–j**) (Table 1; Fig. 2) were synthesized by the acetylation of Schiff base with different substituents. The desired synthesized nicotinyl derivatives was achieved in good yield by reacting aromatic aldehydes i.e., benzaldehyde (**4a**), dimethylaminobenzaldehyde (**4b**), 2-chlorobenzaldehyde (**4c**), 2-nitrobenzaldehyde (**4d**), 4-methoxybenzaldehyde (**4e**), 3-chloro-4-nitrobenzaldehyde (**4f**), 3-nitrobenzaldehyde (**4g**), 4-hydroxy-3-methoxybenzaldehyde (**4h**), 4-methylbenzaldehyde (**4i**), and 3,4-dimethoxybenzaldehyde (**4j**) with

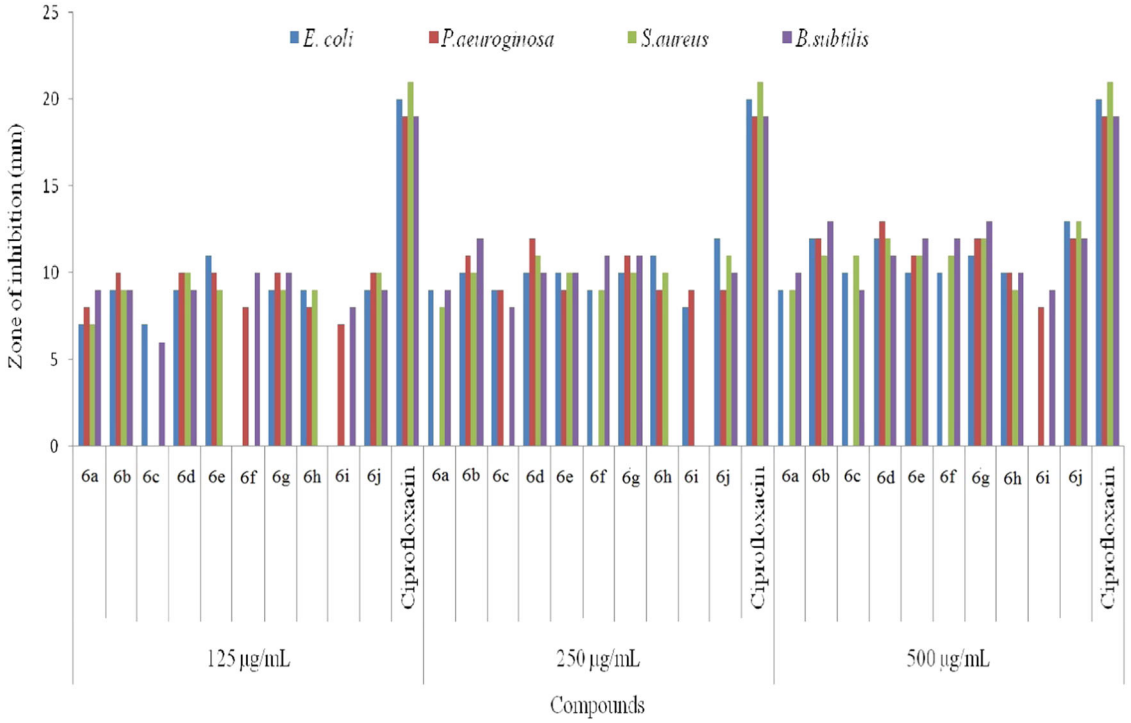

Fig. 3 Antibacterial activity of nicotinic acid derivatives (**6a–j**)

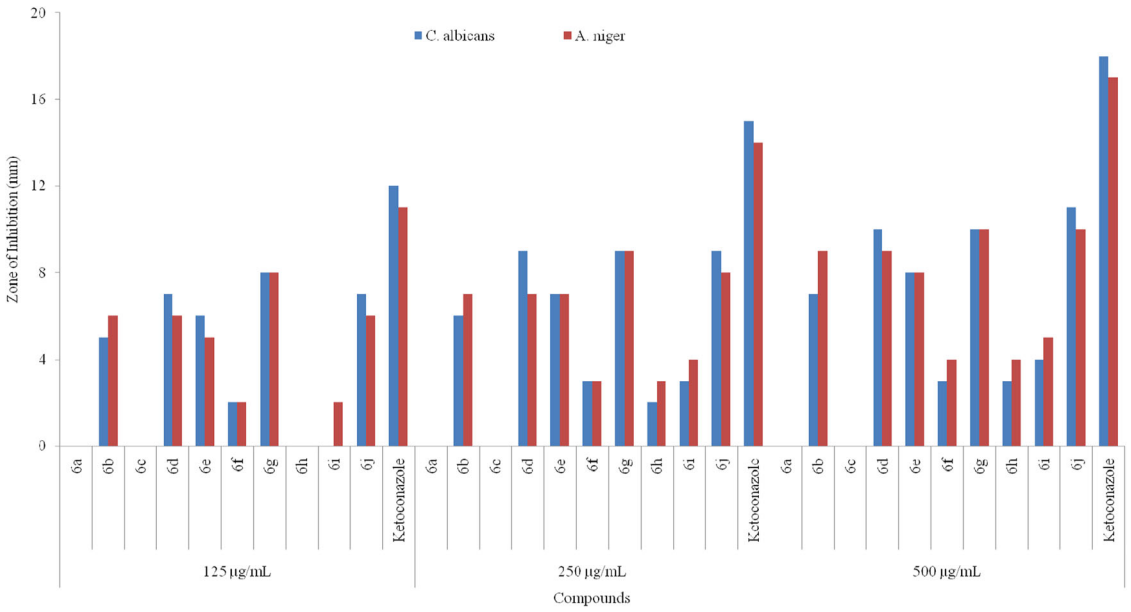

Fig. 4 Antifungal activity of nicotinic acid derivatives (**6a–j**)

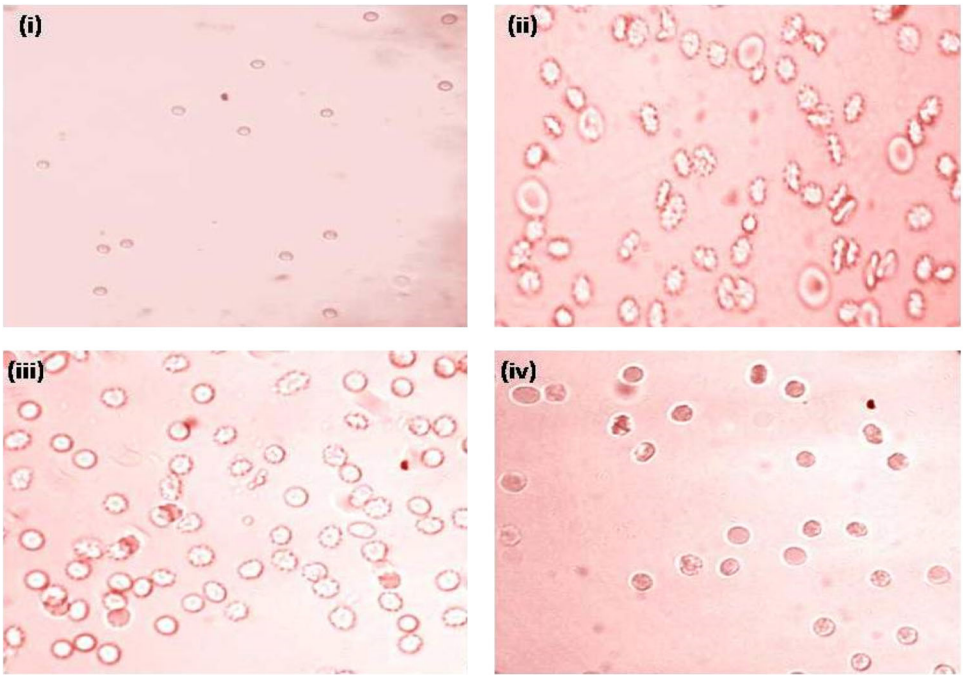

Fig. 5 Erythrocytes photographs (400×) showing surface morphology under influence of **i** normal saline, **ii** ciprofloxacin, **iii** ketoconazole, and **iv** compound **6g** (1 mg/mL)

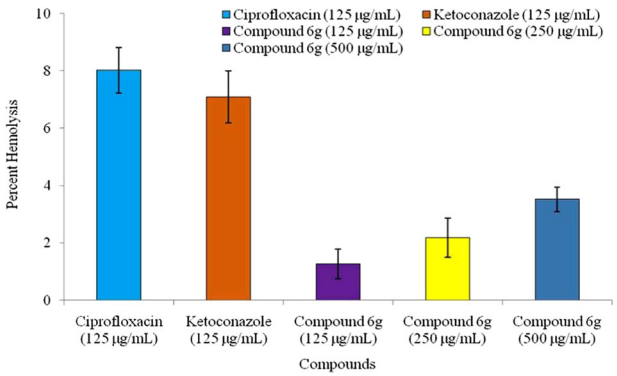

Fig. 6 Hemolytic toxicity profile of different compounds. Results are represented as mean ± SD ($n = 6$)

nicotinoyl hydrazide in ethanol and acetic anhydride (Scheme 1). The nicotinic acid was converted to nicotinoyl chloride by refluxing with phosphorus pentachloride (PCl_5) in carbon tetrachloride (CCl_4) and thereafter it was reacted with hydrazine at low temperature to afford nicotinoyl hydrazide. The synthesized derivatives were characterized by elemental analysis, mass, IR, and NMR spectroscopy.

Antibacterial and antifungal activity

The in vitro antimicrobial activities of all synthesized derivatives (**6a–j**) were performed by cup-plate method using various bacterial strains like *Staphylococcus aureus*, *Bacillus subtilis*, *Escherichia coli*, and *Pseudomonas aeruginosa*, (Fig. 3) as well as fungal strains like *Candida albicans and Aspergillus niger* in terms of zone of inhibition (Fig. 4). At the selected maximum concentration (500 µg/mL), compounds **6a**, **6b**, **6e**, **6f**, **6g**, and **6i** exhibited maximum zone of inhibition (antibacterial activity) against *B. subtilis*. Apart from this compounds **6c** and **6d** displayed maximum zone of inhibition against *S. aureus* and *P. aeuroginosa*, respectively at concentration of 500 µg/mL while compound **6j** exhibited similar antibacterial activity against other strain of bacteria i.e., *E. coli* and *S. aureus* at

Table 3 Molecular docking study of synthesized compounds (**6a–j**)

Entry	Compounds	Binding affinity (Kcal/mol)		
		Antimicrobial 2xct	Antifungal 3gw9	Antitubercular 3hnt
1	**6a**	−8.3	−7.1	−6.4
2	**6b**	−8.7	−8.0	−6.4
3	**6c**	−8.3	−7.1	−6.5
4	**6d**	−8.3	−7.7	−6.1
5	**6e**	−8.5	−7.6	−6.4
6	**6f**	−9.5	−8.6	−6.6
7	**6g**	−9.9	−8.0	−6.6
8	**6h**	−8.4	−7.8	−6.4
9	**6i**	−7.8	−8.4	−6.5
10	**6j**	−9.0	−8.4	−6.5
11	Ciprofloxacin	−10.4	–	–
12	Ketoconazole	–	−8.5	–
13	Rifampicin	–	–	−6.8

the 500 µg/mL concentration. Interestingly, compounds **6h** and **6i** showed maximum antibacterial activity against *E. coli* and *P. aeuroginosa*, respectively at concentration of 250 µg/mL (Fig. 3).

Further, all synthesized compounds (**6a–j**) were also evaluated for in vitro antifungal activity against selected fungi i.e., *C. albicans* and *A. niger*. At the concentration of 500 µg/mL, compounds **6d** and **6j** exhibited maximum antifungal activity against *C. albicans* while compounds **6b**, **6f**, **6h**, and **6i** exhibited maximum zone of inhibition against *A. niger*. Interestingly, compounds **6e** and **6g** showed similar antifungal activity against both, *C. albicans* and *A. niger*. The compounds **6a** and **6c** were devoid of any antifungal activity at various tested concentrations ranging from 125 to 500 µg/mL (Fig. 4).

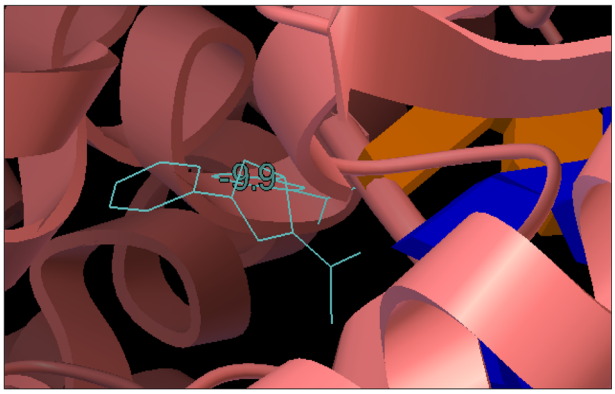

Fig. 7 Interaction of **6g** (blue color) as an antimicrobial on protein 2xct (DNA gyrase) in line model (6g) ribbon structure (2xct) (color figure online)

For investigating the antitubercular activity, all the synthesized compounds **6a–j** were screened against *M. tuberculosis H37Rv* strain. The result of antitubercular activity is represented in Table 2 in terms of % inhibition and MIC values. All the compounds revealed significant inhibitory activity against *M. tuberculosis* H37Rv at 100 µg/mL with 100% inhibition except compounds **6e** and **6i**, which showed less than 90% inhibition. The compounds substituted with nitro groups (**6f**, **6g**, and **6d**) showed higher antitubercular activity as compared to other compounds. Out of all the synthesized derivatives, compounds **6f**, **6g**, and **6d** exhibited excellent antitubercular activity with MIC values of 1.2, 3.1, and 7.8 µg/mL, respectively. The position of nitro substituent greatly affected the antitubercular activity (Lourenço et al. 2007; Kamanna and Kashyap 2007). The nitro group at *para* position (compound **6f**) showed more potency than others.

Normally, human erythrocytes are regular biconcave disks and the deformability of normal human erythrocytes geometry affects their ability to survive in the microcirculation. The toxicity of synthesized nicotinic acid derivatives were evaluated by observing the changes in surface morphology of erythrocytes, which reflected the toxicity. All the compounds were studied at the concentration of 1 mg/mL. The erythrocytes cells displayed lesser

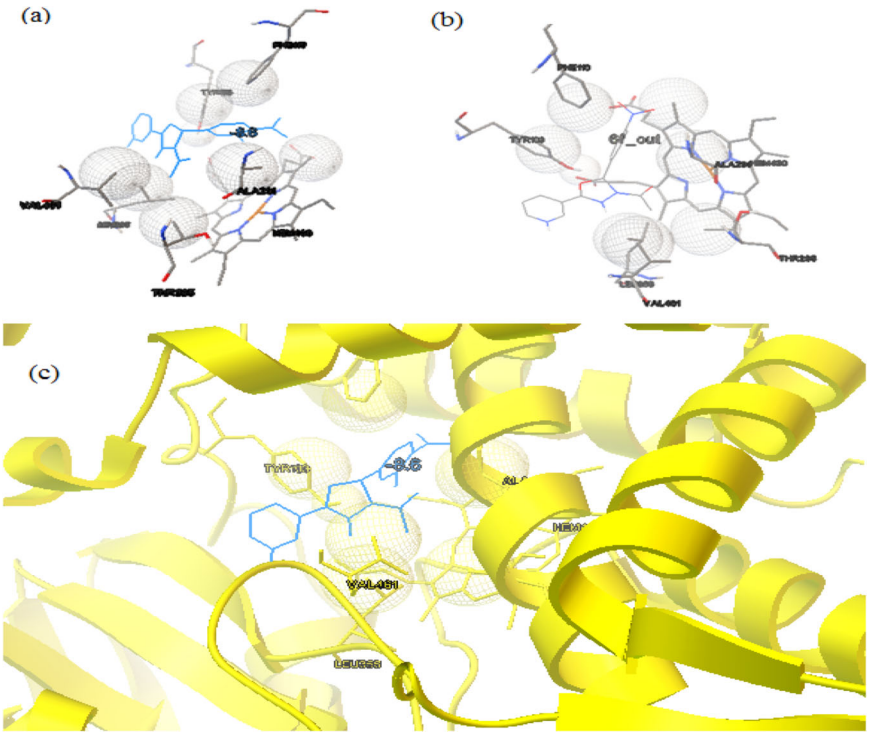

Fig. 8 The interaction of **6f** (blue color) as an antifungal on protein 3gw9 in ball and stick model (**a**, **b**) and ribbon structure (**c**) (color figure online)

deformities in shape as compared with normal saline control group as shown in Fig. 5. The compound **6g** caused least deformation to the erythrocytes as compared to the standard ciprofloxacin and ketoconazole.

Along with the changes in contour of RBCs, the hemolysis of erythrocytes was also studied. Erythrocytes lysis is an easy method to study any possible interaction between synthesized compound and RBCs membrane. This can provide qualitative as well as quantitative indication of potential damage to RBCs by administered compound. It gives a quantitative measure of hemoglobin (Hb) release (Mishra et al. 2010; Mishra and Jain 2014). The compound **6g** exhibited significantly very less hemolytic toxicity at different concentrations i.e., 125, 250, and 500 µg/mL as compared to the standards ciprofloxacin and ketoconazole at concentration of 125 µg/mL (Fig. 6).

On the basis of effects on surface morphology of erythrocytes and hemolytic toxicity investigations, it could be concluded that the synthesized compounds exhibited negligible toxicity, which advocated that the synthesized acetylated nicotinic acid derivatives could be developed for exploring its further biomedical applications.

Molecular docking studies

For the identification of molecular interaction and insight mechanism all the synthesized compounds **6a–j** were screened by Autodock Vina 1.5.6 software (version 1.5.6, The SCRIPPS Research Institute, Germany) (Trott and Olson 2010). The proteins PDB 2xct, 3gw9 and 3hnt were downloaded from protein data bank (http://www.rcsb.org/pdb/home/home.do). The structures of the compounds were drawn by ChemBioDrwa Ultra 12.0 (CambridgeSoft) and converted to 3D structures. Energy minimizations and geometry optimization were performed by MM2 Interface program on ChemBio3D Ultra 12.0. Further the interactions of these compounds were evaluated on 2xct (DNA gyrase),

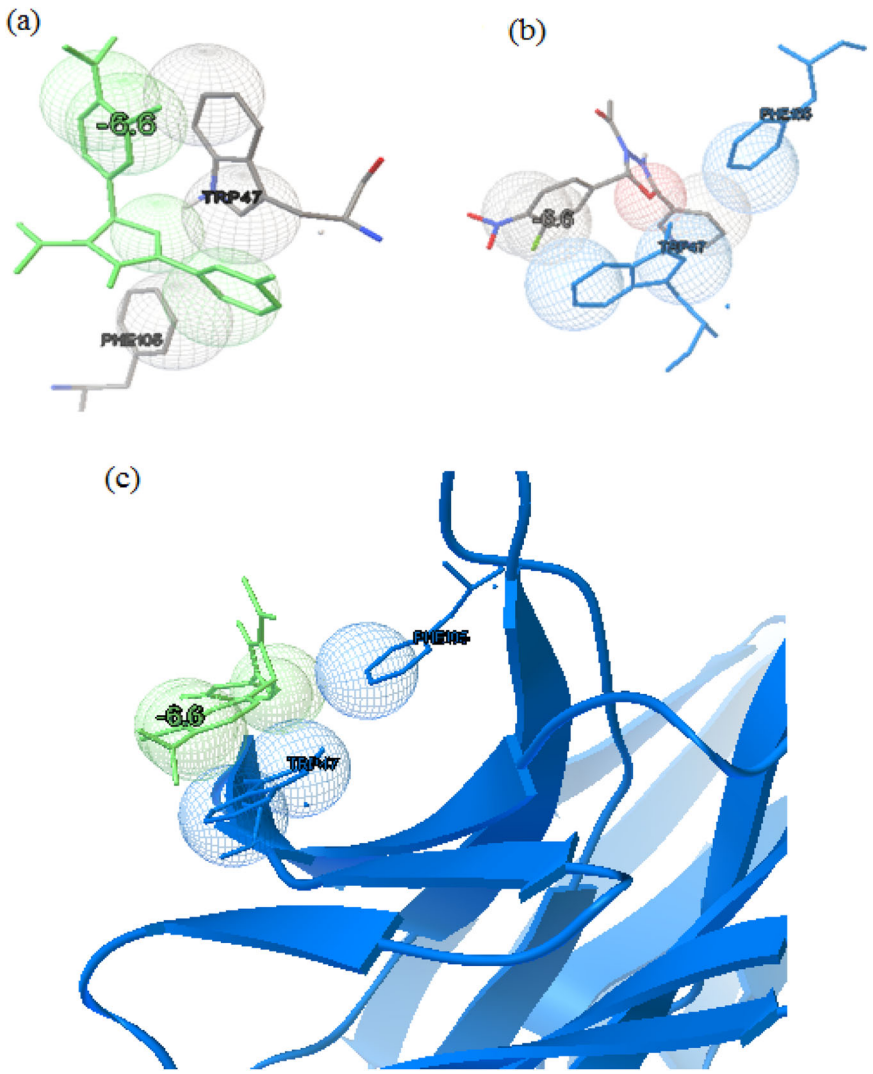

Fig. 9 The interaction of **6f** (green color) as an antitubercular with 3hnt protein (**a**, **b**) and ribbon structure (**c**)

3gw9 and 3hnt protein for the antimicrobial, antifungal and antitubercular activity, respectively.

The results of binding affinity obtained by molecular docking are shown in Table 3. The binding affinity correlates with their in vitro activity. In-depth analysis was done for the compounds, which showed the best activity in in vitro assay as well as good binding affinity in molecular docking study. Among the all, compound **6g** showed better binding affinity (−9.9 Kcal/mol) as compared to that of the ciprofloxacin (−10.4 Kcal/mol; entry 7, Table 3). Similarly compound **6g** showed good in vitro antimicrobial activity against *S. aureus* and *P. aeuroginosa* at concentration of 500 µg/mL. The interaction of compound **6g** with protein 2xct (DNA gyrase), the binding site was shown in Fig. 7.

Under in vitro antifungal activity the compounds **6b**, **6f**, **6h**, and **6i** exhibited maximum zone of inhibition and good binding affinity to 3gw9 protein. The compound **6f** compound has good binding affinity (−8.6 Kcal/mol), which was comparable to ketoconazole (−8.5 Kcal/mol) (entry 6, Table 3). The interaction of compound **6f** with 3hnt protein was depicted in Fig. 8 showing hydrophobic interaction of compound **6f** with various amino acid residues i.e., PHE110, TYR109, THR214, VAL461 at binding site.

The compounds substituted with nitro groups (**6f**, **6g**, and **6d**) showed higher in vitro antitubercular activity and same was reflected in the binding affinity obtained from molecular docking. The compound **6f** with *para* nitro group showed more potency and high binding affinity (−6.6 Kcal/mol; entry 6, Table 3). In-depth binding interaction for **6f** compound (Fig. 9), showed hydrophobic interaction with various amino acid residues i.e., PHE105, TRP47 at binding site.

Conclusion

The acetylated nicotinic acid derivatives (**6a–j**) were synthesized by four step methodology. These synthesized compounds exhibited superior antimicrobial, antifungal, and antitubercular activities. Among all, the compounds **6b**, **6d**, **6e**, **6g**, and **6j** demonstrated excellent antimicrobial activity. The methoxy and nitro group substituted compounds (**6e**, **6j** and **6d**, **6g**) showed higher antimicrobial, antifungal, and antitubercular activity and their position also affected activity. The nitro group at *p*-position (compound **6g**), potentiated the biological activity. These compounds were studied by molecular docking through Autodock Vina to evaluate the interaction of these compounds at respective proteins. On the basis of different hopeful results, it can be concluded that the potential for further structural fine-tuning renders compound **6g** as a promising lead compound for the development of new drugs for the treatment of TB as well as fungal infection.

Acknowledgements Authors are obliged to Sophisticated Analytical Instrument Facility, Indian Institute of Technology, Chennai, India for IR, NMR and mass spectroscopy of compounds.

Compliance with ethical standards

Conflict of interest The authors declare that they have no competing interests.

References

Boovanahalli SK, Jin X, Jin Y, Kim JH, Dat NT, Hong YS, Lee JH, Jung SH, Lee K, Lee JJ (2007) Synthesis of (arylox-yacetylamino)-isonicotinic/nicotinic acid analogs as potent hypoxia inducible factor (HIF)-1α inhibitors. Bioorg Med Chem Lett 17:6305–6310

Caminero JA, Sotgiu G, Zumla A, Migliori GB (2010) Best drug treatment for multidrug-resistant and extensively drug-resistant tuberculosis. Lancet Infect Dis 10:621–629

Chaurasiya S, Kaur P, Nayak SK, Khatik GL (2016) Virtual screening for identification of novel potent EGFR inhibitors through Autodock Vina molecular modeling software. J Chem Pharm Res 8:353–360

Desai NC, Bhavsar AM, Shah MD, Anil SK (2008) Synthesis and QSAR studies of thiosemicarbezides, 1,2,4-triazole, 1,2,3-thiadaizoles and 1,3,4-oxadiazoles derivatives as potential antibacterial agents. Indian J Chem 47:579–589

Jo YW, Im WB, Rhee JK, Shim MJ, Kim WB, Choi EC (2004) Synthesis and antibacterial activity of oxazolidinones containing pyridine substituted with heteroaromatic ring. Bioorg Med Chem 12:5909–5915

Kalia R, Rao CM, Kutty NG (2007) Synthesis and evaluation of the anti-inflammatory activity of N-[2-(3,5-Ditert-butyl-4-hydroxyphenyl)-4-oxothiazolidin-3-yl] nicotinamide. Arzneimittel-Forschung-Drug Res 57:616–622

Kamanna VS, Kashyap ML (2007) Nicotinic acid (niacin) receptor agonizts: will they be useful therapeutic agents? Am J Cardiol 100:53N–61N

Kaur P, Khatik GL (2016) Identification of novel 5-styryl-1,2,4-oxadiazole/triazole derivatives as the potential anti-androgens through molecular docking study. Int J Pharm Pharm Sci 8:72–77

Khatik GL, Kaur J, Kumar V, Tikoo K, Nair VA (2012) 1, 2, 4-Oxadiazoles: a new class of anti-prostate cancer agents. Bioorg Med Chem Lett 22:1912–1916

Khatik GL, Kaur J, Kumar V, Tikoo K, Venugopalan P, Nair VA (2011) Aldol derivatives of thioxoimidazolidinones as potential anti-prostate cancer agents. Eur J Med Chem 46:3291–3301

Lourenço MCS, De Souza MNV, Pinheiro AC, Ferreira MDL, Gonçalves RSB, Nogueira TCM, Peralta MA (2007) Evaluation of anti-tubercular activity of nicotinic and isoniazid analogs. ARKIVOC 15:181–191

Mishra V, Gupta U, Jain NK (2010) Influence of different generations of poly(propylene imine) dendrimers on human erythrocytes. Pharmazie 65:891–895

Mishra V, Jain NK (2014) Acetazolamide encapsulated dendritic nano-architectures for effective glaucoma management in rabbits. Int J Pharm 461:380–390

Navarrete-Vázquez G, Molina-Salinas GM, Duarte-Fajardo ZV, Vargas-Villarreal J, Estrada-Soto S, González-Salazar F, Hernández-Núñez E, Said-Fernández S (2007) Synthesis and antimycobacterial activity of 4-(5-substituted-1,3,4-oxadiazol-2-yl) pyridines. Bioorg Med Chem 15:5502–5508

Nookala L, Subash V (2013) Tuberculosis—an overview. Int J Curr Pharm Clin Res 3:77–88

Pandey VK, Gupta VD, Upadhyay M, Upadhyay M, Singh VK, Tandon M (2005) Synthesis, characterization and biological activities of 1,3,4-substituted 2-azetidinones. Indian J Chem 44B:158–162

Punkvang A, Saparpakorn P, Hannongbua S, Wolschann P, Beyer A, Pungpo P (2010) Investigating the structural basis of arylamides to improve potency against M. tuberculosis strain through molecular dynamics simulations. Eur J Med Chem 45:5585–5593

Slayden RA, Lee RE, Barry III CE (2000) Isoniazid affects multiple components of the type II fatty acid synthase system of Mycobacterium tuberculosis. Mol Microbiol 38: 514–525

Trott O, Olson AJ (2010) AutoDock Vina: improving the speed and accuracy of docking with a new scoring function, efficient optimization, and multithreading. J Comput Chem 31:455–461

World Health Organization (WHO) (2015) www.who.int/tb/publications/global_report/en/, Accessed 25 March 2017. www.rcsb.org/pdb/home/home.do, Accessed 11 March 17